THE JOURNAL OF BIOLOGICAL CHEMISTRY
Vol. 277, No. 31, Issue of August 2, pp. 28088–28098, 2002

Printed in U.S.A.

Is the Glycolytic Flux in *Lactococcus lactis* Primarily Controlled by the Redox Charge?

KINETICS OF NAD^+ AND NADH POOLS DETERMINED *IN VIVO* BY ^{13}C NMR*[S]

Received for publication, March 16, 2002, and in revised form, April 29, 2002
Published, JBC Papers in Press, May 13, 2002, DOI 10.1074/jbc.M202573200

Ana Rute Neves‡§, Rita Ventura‡, Nahla Mansour¶‖, Claire Shearman¶, Michael J. Gasson¶, Christopher Maycock‡, Ana Ramos‡§, and Helena Santos‡**

From the ‡Instituto de Tecnologia Química e Biológica, Universidade Nova de Lisboa and Instituto de Biologia Experimental e Tecnológica, Rua da Quinta Grande, 6, Apt 127, 2780-156 Oeiras, Portugal and ¶Institute of Food Research, Norwich Laboratory, Norwich Research Park, Colney, Norwich NR4 7UA, United Kingdom

The involvement of nicotinamide adenine nucleotides (NAD^+, NADH) in the regulation of glycolysis in *Lactococcus lactis* was investigated by using ^{13}C and ^{31}P NMR to monitor *in vivo* the kinetics of the pools of NAD^+, NADH, ATP, inorganic phosphate (P_i), glycolytic intermediates, and end products derived from a pulse of glucose. Nicotinic acid specifically labeled on carbon 5 was synthesized and used in the growth medium as a precursor of pyridine nucleotides to allow for *in vivo* detection of ^{13}C-labeled NAD^+ and NADH. The capacity of *L. lactis* MG1363 to regenerate NAD^+ was manipulated either by turning on NADH oxidase activity or by knocking out the gene encoding lactate dehydrogenase (LDH). An LDH^- deficient strain was constructed by double crossover. Upon supply of glucose, NAD^+ was constant and maximal (~5 mM) in the parent strain (MG1363) but decreased abruptly in the LDH^- strain both under aerobic and anaerobic conditions. NADH in MG1363 was always below the detection limit as long as glucose was available. The rate of glucose consumption under anaerobic conditions was 7-fold lower in the LDH^- strain and NADH reached high levels (2.5 mM), reflecting severe limitation in regenerating NAD^+. However, under aerobic conditions the glycolytic flux was nearly as high as in MG1363 despite the accumulation of NADH up to 1.5 mM. Glyceraldehyde-3-phosphate dehydrogenase was able to support a high flux even in the presence of NADH concentrations much higher than those of the parent strain. We interpret the data as showing that the glycolytic flux in wild type *L. lactis* is not primarily controlled at the level of glyceraldehyde-3-phosphate dehydrogenase by NADH. The ATP/ADP/P_i content could play an important role.

Lactococcus lactis plays an essential role in the manufacture of a wide range of dairy products. The relative simplicity of *L. lactis* metabolism that converts sugars via the glycolytic pathway to pyruvate, generating energy mainly through substrate level phosphorylation, makes it an attractive model organism to test metabolic engineering strategies. Moreover, the large number of genetic tools available for *L. lactis* (1) and the recent release of the complete genome sequence are additional incentives to study the physiology of this organism in great depth (2).

Despite numerous studies, a satisfactory answer to the question, What controls the glycolytic flux in *L. lactis*? has not been put forward. During homolactic fermentation, regulation of the carbon flux has been associated with high levels of fructose 1,6-bisphosphate (FBP),[1] which activates lactate dehydrogenase (LDH; EC 1.1.1.27) and pyruvate kinase (PK; EC 2.7.1.40), directing the flux toward the production of lactate (3). A metabolic shift from homolactic (lactate production) to mixed acid fermentation (ethanol, acetate, and formate production) was observed in glucose-limited chemostat cultures (4). A deviation from homolactic fermentation was also reported under aerobic conditions (5) or during the metabolism of galactose (6). The formation of end products other than lactate in glucose-limited cultures was rationalized as being due to the reduction of LDH activity caused by lower levels of the effector, FBP, and to the relief of pyruvate formate lyase inhibition by the concomitant decrease of dihydroxyacetone phosphate and glyceraldehyde 3-phosphate; on the other hand, the oxygen-induced metabolic shift would be explained by activation of the pyruvate dehydrogenase complex under aerobic conditions (3). Recently, Garrigues *et al.* (7) downplayed the role of FBP, proposing that control of glycolysis was dependent on modulation of glyceraldehyde-3-phosphate dehydrogenase (GAPDH; EC 1.2.1.12) by $NADH/NAD^+$ (7), and earlier work based on inhibitor titrations also suggests GAPDH as a major site for glycolytic control (8).

L. lactis shows a remarkable versatility in regard to metabolic routes used to regenerate NAD^+, a crucial process in this typical fermentative organism. The presence of NADH oxidase activity enables this organism to utilize oxygen, when available in the environment, as an acceptor for the reducing power in NADH, inducing a shift of the carbon flux to the production of

* This work was supported by Commission of the European Communities Contracts BIO4CT-96-0498 and QLK1-CT-2000-01376 and by Fundação para a Ciência e Tecnologia, Portugal, Contract PRAXIS/P/BIA/11072/1998. The costs of publication of this article were defrayed in part by the payment of page charges. This article must therefore be hereby marked "*advertisement*" in accordance with 18 U.S.C. Section 1734 solely to indicate this fact.

[S] The on-line version of this article (available at *http://www.jbc.org*) contains Supplemental Figs. 1 and 2.

§ Supported by research fellowships of Fundação para a Ciência e Tecnologia, Portugal.

‖ Supported by a Ph.D. studentship from the Egyptian Government and National Research Centre. Current address: Food Science and Dairy Technology, National Research Centre, Tahir St., Cairo, Egypt.

** To whom correspondence should be addressed: Instituto de Tecnologia Química e Biológica, Universidade Nova de Lisboa, Rua da Quinta Grande, 6, Apt 127, 2780-156 Oeiras, Portugal. Tel.: 351-21-4469828; Fax: 351-21-4428766; E-mail: santos@itqb.unl.pt.

[1] The abbreviations used are: FBP, fructose 1,6-bisphosphate; Mtl1P, mannitol 1-phosphate; PEP, phosphoenolpyruvate; 3-PGA, 3-phosphoglycerate; P_i, inorganic phosphate; KP_i, potassium phosphate; LDH, L-lactate dehydrogenase; LDH^-, LDH-deficient strain; GAPDH, glyceraldehyde-3-phosphate dehydrogenase; PK, pyruvate kinase; Mes, 2-(*N*-morpholino)ethanesulfonic acid; PIPES, piperazine-*N*,*N*′-bis(2-ethanesulfonic acid).

acetate and acetoin (9). On the other hand, mutants with disruption of LDH, the main catalytic site for NAD^+ regeneration, produced mannitol or ethanol as alternatives to lactate (10, 11).

The ubiquitous role of pyridine nucleotides in the energy-transforming and redox reactions and their potential involvement in regulation of carbon fluxes has demanded the determination of the intracellular levels of NAD^+ and NADH. However, reliable data on intracellular pools of NAD^+ and NADH are hard to obtain. Most studies rely on analysis of cell extracts, which may not represent the composition of living cells in a specific metabolic state due to compound instability and/or unsatisfactory quenching of metabolism. NADH and NAD^+ are acid and alkali labile, respectively, and we found that NADH was not fully stable under ethanol extraction conditions. Therefore, measurement of both oxidized and reduced forms requires that extraction be carried out in separate samples, with consequent impairment of reproducibility. These are probably the most important factors responsible for the discrepancies found in the literature for NAD^+ and NADH concentrations in *L. lactis* (12–15) and other organisms (16–21).

Therefore, the development of techniques for monitoring these pools in a non-invasive way is mandatory. The fluorescence of NAD(P)H has been used for the characterization of intracellular pyridine nucleotide metabolism (22), but this methodology has the disadvantage of detecting the reduced forms only, and data obtained with this technique in whole cells should be regarded as qualitative rather than quantitative (Ref. 23 and references therein).

In vivo ^{13}C NMR was used by Unkefer *et al.* to follow pyridine nucleotide metabolism in *Escherichia coli* and yeast cells (24). The ability of this method to monitor both the reduced and oxidized pools non-invasively allied to the concomitant observation of intracellular metabolites derived from ^{13}C substrates is expected to provide a more comprehensive and reliable insight into cell metabolism. In this study, we used this methodology to monitor the kinetics of the intracellular pools of NAD^+, NADH, and several metabolic intermediates in the living cells of *L. lactis* without interfering with the cellular processes. Manipulation of the cell capacity to regenerate NAD^+ was achieved either by turning on NADH oxidase activity (switching from anaerobic to aerobic conditions) or by knocking out the gene encoding lactate dehydrogenase, the main site for NADH oxidation in this organism. Regulation of glycolysis in *L. lactis* is discussed in the light of these *in vivo* measurements.

MATERIALS AND METHODS

Microbial Strains and Growth Conditions—L. lactis MG1363 (parent strain) and FI9630, harboring an *ldh* gene deletion, hereafter denoted as LDH^- strain, were grown at 30 °C in a 2-liter vessel (B. Braun Biostat® MD) in the chemical-defined medium described by Poolman and Konings (25) modified as follows. Aspartate and asparagine were omitted, and nicotinic acid (1 mg/liter) was replaced by [5-^{13}C]nicotinic acid (5 mg/liter). Glucose was added to a final concentration of 1% (w/v), and the pH was kept at 6.5 by automatic addition of 10 N NaOH. Anaerobiosis was attained by flushing sterile argon through the medium in the fermenter for 1 h preceding inoculation. Dissolved oxygen was monitored with an oxygen electrode (Ingold). A specific air tension of 90% was maintained by automatic control of the airflow during aerobic growth.

Construction of an LDH^- Strain by Double Crossover (FI9630)—An *L. lactis* LDH-deficient strain was constructed by double crossover to ensure full stability of the gene knock-out and to avoid antibiotic selection. The pOri/pVE6007 two-plasmid system (26) was used to generate a food grade deletion of the *ldh* gene in MG1363. The upstream flanking fragment was cloned from pFI2320 as a 1.24-kb *Eco*RI-*Dra*I fragment (equivalent to 1785–3025 bp; accession number L07920 (27)). This fragment was cloned into pOri280 cut with *Eco*RI and *Sma*I to give pFI2277. The DNA sequence downstream of the *ldh* gene was determined from pFI516 (28) and used to design primers ldh3 (5′-CCGTCAGCCCGCGGCGCAATTGC-3′) and ldh4 (5′-GCAATCAAAGCTTCAGAAGCC-3′). These primers amplified the 950-bp downstream fragment, which was cloned into $pCR^{2.1}$TOPO (Invitrogen) to give pFI2323. pFI2277 was cut with *Bgl*II, and the 1.98-kb *Bam*HI-*Bgl*II fragment from pFI2323 was inserted. The orientation of the upstream and downstream *ldh* fragments was confirmed by PCR analysis and sequencing across the junction. This construct, named pFI2278, was electroporated into FI8645 (MG1363 pVE6007) to give FI9619. This strain was taken through the temperature shift protocol for single and double crossovers (26), giving FI9620 and FI9630, respectively. FI9630 was confirmed as a Δ*ldh* strain by PCR analysis, Southern blotting, and sequencing of the PCR product amplified across the deletion junction. The stability of the LDH deletion was assessed as described previously (10).

Synthesis of [5-^{13}C]Nicotinic Acid—[5-^{13}C]Nicotinic acid was synthesized starting from [1,3-^{13}C]acetone (Cambridge Isotope Laboratories, MA) and *o*-aminobenzaldehyde. A modification of the method previously used to prepare [6-^{13}C]nicotinamide was followed (29). Base-catalyzed condensation of *o*-aminobenzaldehyde and [1,3-$^{13}C_2$]acetone afforded labeled quinaldine in 90% yield. Bromination was carried out as described in Vogel (30), also in high yield (96%), to produce tribromoquinaldine. The alternative method for this bromination (29) was not satisfactory in our hands. Hydrolysis of the tribromomethyl group was performed by heating in sulfuric acid until no more bromine vapors were observed. Oxidative degradation of the resulting acid with nitric acid had to be carried out under very careful control in a temperature-controlled oil bath. Heating below 260 °C resulted in the formation of several products, and heating even marginally above this temperature resulted in the formation of several products or the complete carbonization of the product. The acidic residue from this reaction was heated in the presence of methanol and trimethylorthoformate for 18 h to give the required diester in 75% yield for the two steps. Selective hydrolysis of the 2-carboxylate was carried out by refluxing the diester in a solution of potassium hydroxide (1.01 eq.) in methanol. The monoacid (80% yield) formed on acidifying was then decarboxylated by heating to reflux in anisole for 6 h. Without purification, the methyl ester was hydrolyzed by potassium hydroxide in water to yield nicotinic acid, which was extracted from the acidified aqueous phase continuously with dichloromethane. At least two extractions of up to a week were found necessary for optimum yields. Pure nicotinic acid was obtained in 90% overall yield from the monoacid. The overall yield for the entire process was 47%.

NMR Experiments—Cells were harvested in mid-logarithmic growth phase (A_{600} = 2.2), centrifuged, washed twice, and suspended to a protein concentration of 16.5 mg/ml in 50 mM KP_i or Mes/KOH buffer, pH 6.5, for ^{13}C or ^{31}P NMR experiments, respectively. To determine whether the metabolism was affected by the presence or absence of phosphate in the buffer, experiments using PIPES for ^{13}C NMR were also run. No changes in the dynamics and levels of intracellular metabolites, namely FBP, phosphoenolpyruvate (PEP), and 3-phosphoglycerate (3-PGA) were observed when PIPES instead of KP_i was used (data not shown). Anaerobic experiments were performed as described before (31). For experiments under O_2 atmosphere, a micro pO_2 probe (Lazar Research Laboratories, Inc.) was included in the experimental set-up previously described (31). To ensure an adequate level of oxygenation, an air-lift system (32) with pure oxygen was used inside the NMR tube, and in addition, pure oxygen was continuously bubbled through the cell suspension in the bioreactor. Spectra were acquired sequentially before and after addition of [1-^{13}C]glucose (40 or 80 mM). After glucose exhaustion and when no changes in the resonances due to end products and intracellular metabolites were observed, an aliquot of the cell suspension was passed through a French press; the resulting cell extract was incubated at 80 °C (10 min) in a stoppered tube, cooled down on ice, and cell debris and denatured macromolecules were removed by centrifugation. The supernatant, designated herein as NMR sample extract, was used for quantification of end products and minor metabolites as previously described (10). Although individual experiments are illustrated in each figure, each type of *in vivo* NMR experiment was repeated at least twice, and the results were highly reproducible. The values reported are averages of 2–4 experiments, and the accuracy varied from 2% (end products) to 15% in the case of intracellular metabolites with concentrations below 5 mM.

Preparation of Ethanol Extracts for Purification, Identification, and Quantification of Intracellular [5-^{12}C]NAD^+—A cell suspension of *L. lactis* MG1363 grown under anaerobiosis was prepared as described for *in vivo* NMR, except that ~1 g of cells was suspended in a volume of 60 ml in ultrapure water. The suspension was transferred to 1.2 liters of cold ethanol 70% (v/v) and extracted as described by Ramos *et al.* (33). During the extraction procedure, the pH was kept below 7.5 to avoid

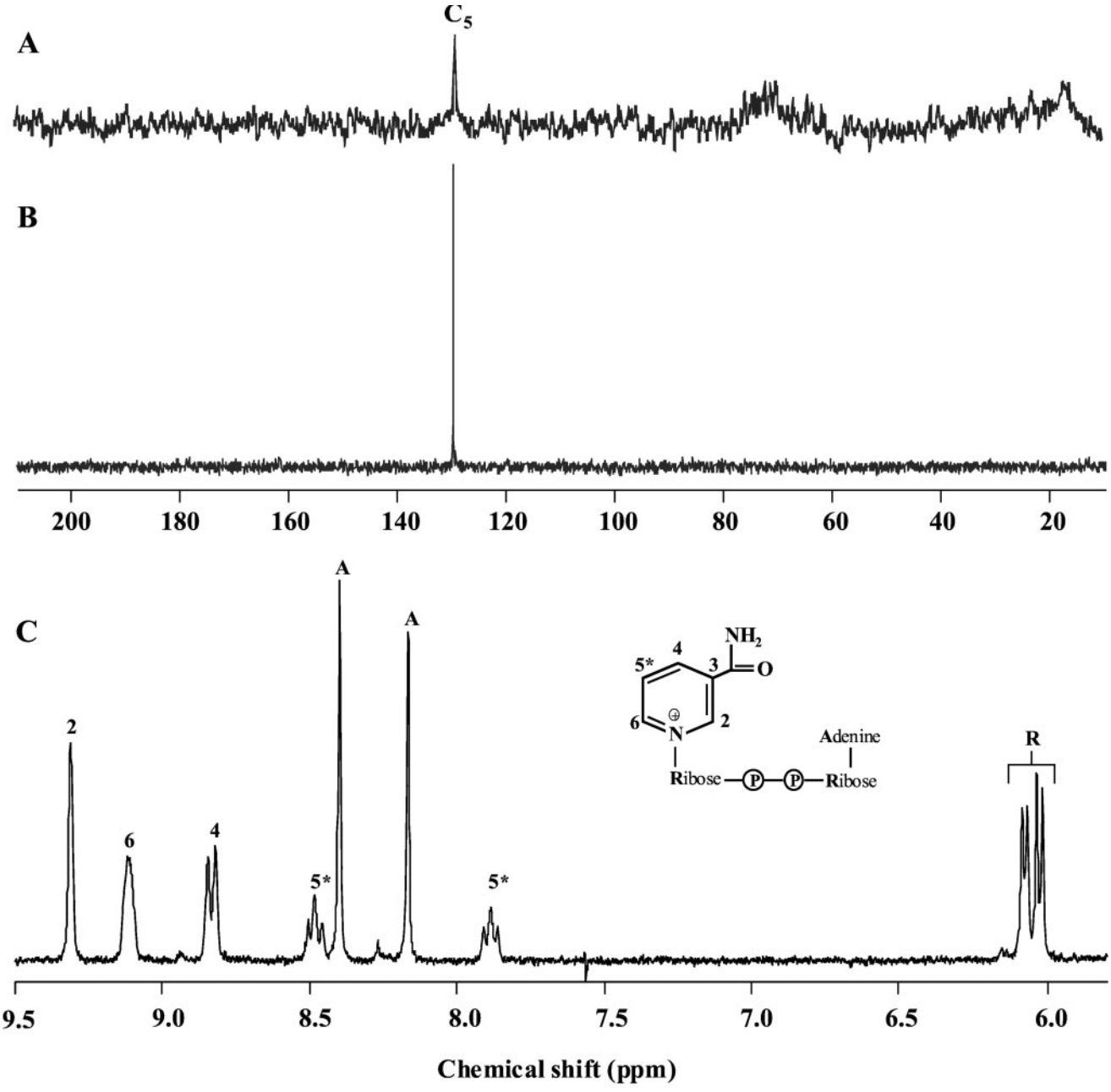

FIG. 1. **^{13}C NMR spectrum of an anaerobic suspension of *L. lactis* cells grown in the presence of [5-^{13}C]nicotinic acid (*A*); carbon (*B*) and proton (*C*) spectra of the purified [5-^{13}C]NAD$^+$ at pH 6.5.** The resonance in *spectrum A* is due to the C_5 of NAD$^+$. Resonances labeled with *R* and *A* are assigned to protons in ribose and adenine moieties, respectively.

NAD$^+$ degradation. To substantiate the assignment to [5-^{13}C]NAD$^+$ of the resonance at 129.1 ppm observed in the ^{13}C NMR spectrum of *L. lactis* before substrate addition, cell components present in the extract were separated by anion-exchange chromatography, the extract was loaded onto a QAE-Sephadex column equilibrated with 5 mM acetate buffer, pH 6.0, and the elution was performed with a linear gradient of 5 mM to 1 M acetate buffer, pH 6.0. Aliquots of each fraction were analyzed by ^{13}C NMR, and fractions originating at the resonance at 129.1 ppm eluting between 0.5 and 0.6 M acetate were pooled, lyophilized, and dissolved in ^2H_2O. Assignment of [5-^{13}C]NAD$^+$ was performed by ^{1}H NMR and ^{13}C NMR spectroscopy.

The concentration of [5-^{13}C]NAD$^+$ was also measured in cell extracts by ^{1}H NMR to provide a basis for comparison with *in vivo* determinations. Cell suspensions (anaerobic cultures) were prepared as described for NMR experiments, incubated at 30 °C for 15 min under an argon atmosphere, and extracted with ethanol as above. The lyophilized extracts were dissolved in ^2H_2O containing 5 mM EDTA; the concentration of [5-^{13}C]NAD$^+$ was determined by comparing the areas of its resonance in ^{1}H- or ^{13}C-relaxed spectra with the area of the resonance due to formate or [3-^{13}C]lactate, added as internal standards for analysis by ^{1}H NMR or ^{13}C NMR, respectively.

Quantification of Products—Lactate, acetoin, acetate, 2,3-butanediol, ethanol, and formate were quantified in NMR sample extracts by ^{1}H NMR (10). The concentration of minor products (*e.g.* pyruvate, ethanol, diacetyl) and metabolic intermediates that remained inside the cells (PEP, 3-PGA) was determined from the analysis of ^{13}C spectra of NMR sample extracts as previously described (31). The concentration of labeled lactate determined by ^{1}H NMR was used as a standard to calculate the concentration of the other metabolites in the sample, and the total amount of lactate was confirmed by enzymatic methods.

Quantification of Intracellular Metabolites in Living Cells by ^{13}C NMR—Because of the fast pulsing conditions used for acquiring *in vivo* ^{13}C spectra, correction factors have to be determined to convert peak intensities into concentrations. The correction factor for the C_5 of NAD$^+$ (0.64 ± 0.01) was determined as follows. A cell suspension was prepared as described above for ^{13}C NMR experiments, 2.5 mM [3-^{13}C]lactate was added, and circulation was started. In the absence of glucose, the intensity of the resonance due to C_5 of NAD$^+$ remained constant for a long period of time, enabling the acquisition of fully and partially relaxed spectra and the determination of correction factors. For the

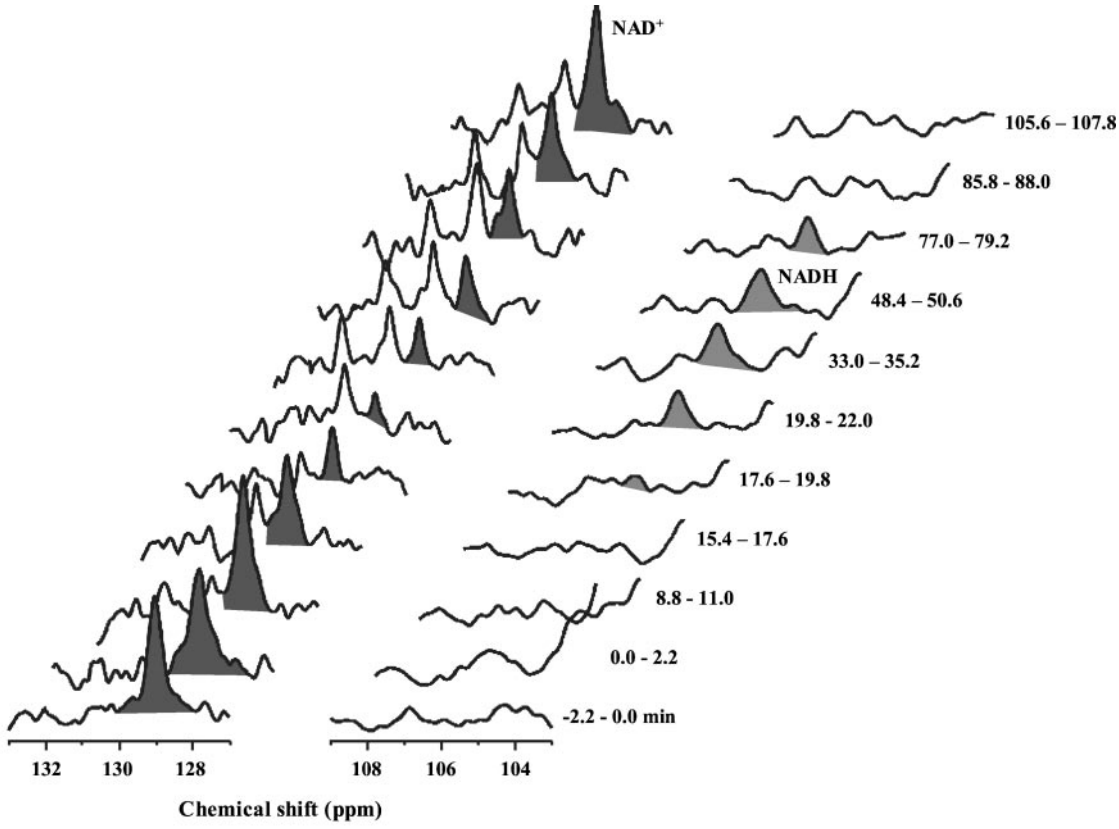

FIG. 2. **Sequence of ^{13}C spectra showing the evolution of NAD^+ (*dark gray*) and NADH (*light gray*) pools in MG1363 before and after the addition of glucose under anaerobic conditions.** Cells were grown in chemical-defined medium containing 5 mg/liter [5-^{13}C]nicotinic acid and suspended in 50 mM KP_i, pH 6.5, at a protein concentration of 16 mg/ml. Glucose (80 mM) was added at time 0; each spectrum was acquired within 2.2 min and processed with 25/35 Hz line-broadening. The two unknown resonances (129.8 and 130.1 ppm) downfield of [5-^{13}C]NAD^+ were assigned to minor products of glucose metabolism.

resonances due to C_1 and C_6 of FBP (0.48 ± 0.02), mannitol, and mannitol 1-phosphate (Mtl1P) (0.48 ± 0.01), the factors were determined from spectra of a perchloric acid extract, which was circulated through the NMR tube at a similar rate to that used for cell suspensions. Extracts were derived from suspensions of LDH^- (Mtl1P and mannitol) or MG1363 cells (FBP) actively metabolizing [1-^{13}C]glucose. The correction factors for the resonances due to C_3 of 3-PGA and PEP (0.60 ± 0.02) were determined in a cell suspension of *L. lactis* after the metabolism of [1-^{13}C]glucose, since after glucose depletion the intracellular pools of these metabolites were stable. The quantitative kinetic data for intracellular metabolites were calculated from the areas of the relevant resonances by applying the correction factors and comparing with the intensity of the lactate resonance in the last spectrum of the sequence. For calculation of the correction factors ^{13}C NMR spectra were acquired with a 60° flip angle and a recycle delay of 0.3 s (saturating conditions) or 60.3 s (relaxed conditions). Average values derived from at least three independent experiments were used. The lower limit for *in vivo* NMR detection of NAD^+ or NADH under these conditions was 0.5 mM. Intracellular metabolite concentrations were calculated using a value of 2.9 μl/mg protein for the intracellular volume of *L. lactis* (34).

NMR Spectroscopy—All NMR spectra of living cells were run at 30 °C with a quadruple-nucleus probe head on a Bruker DRX500 spectrometer. Acquisition of ^{31}P NMR and ^{13}C NMR spectra was performed as described by Neves *et al.* (31); however, acquisition parameters for ^{13}C NMR were modified as follows: data size, 16,000; recycle delay, 0.3 s; number of transients, 480. Carbon and phosphorus chemical shifts are referenced to the resonances of external methanol or H_3PO_4 (85%) designated at 49.3 ppm and 0.0 ppm, respectively.

Enzyme Activity Measurements—All enzymes were assayed at 30 °C immediately after mechanical disruption of a cell suspension by passage through a French press (twice at 120 MPa) and centrifugation for 15 min at 30,000 × *g* to remove cell debris. The protein concentration was determined by the method of Bradford (35). L-LDH was assayed as described by Garrigues *et al.* (7). GAPDH was assayed by the method of Even *et al.* (36). NADH oxidase activity was determined as described by Lopez de Felipe *et al.* (9). Mtl1P dehydrogenase (EC 1.1.1.17), leading to the formation of Mtl1P, was measured using 0.3 mM NADH, and the reaction was initiated by the addition of 3 mM fructose 6-phosphate (10).

Chemicals—[1-^{13}C]Glucose (99% enrichment) and [1,3-^{13}C]acetone (99% enrichment) were obtained from Campro Scientific and Cambridge Isotope Laboratories, respectively. [3-^{13}C]Lactate (99%) was supplied by A.R.C. Formic acid (sodium salt) was purchased from Merck. QAE-Sephadex A25 was obtained from Amersham Biosciences. All other chemicals were reagent grade.

RESULTS

^{13}C Labeling of Intracellular Pools of Pyridine Nucleotides—In most microbial systems NAD^+ can be synthesized from aspartate (*de novo* pathway) or nicotinic acid (salvage pathway) (37). Because of the lack of information about the route of NAD^+ synthesis in *L. lactis*, it was necessary to ascertain which precursor would achieve maximal labeling of the intracellular pool. Therefore, *L. lactis* was grown in chemical-defined medium without nicotinic acid or without aspartate and asparagine. In the absence of these amino acids, a slight decrease in the growth rate (μ) was observed: $\mu = 0.71\ h^{-1}$ as compared with $\mu = 1.15\ h^{-1}$ for the complete chemical-defined medium under anaerobiosis. No growth was detected when nicotinic acid was omitted. These data and the previous observation of the production of labeled aspartate from the metabolism of [1-^{13}C]glucose (10) led to the conclusion that nicotinic acid, but not aspartate, was essential for growth and, therefore, was the compound of choice to supply as a biosynthetic precursor of NAD^+. In this work, aspartate and asparagine were omitted from the medium to ensure maximal labeling of the pyridine nucleotide pool. [5-^{13}C]Nicotinic acid was synthesized, with an overall yield of 47% as described under "Materials and Methods" and used as the only nicotinic acid source for the growth of *L. lactis*. The purity of the labeled compound was

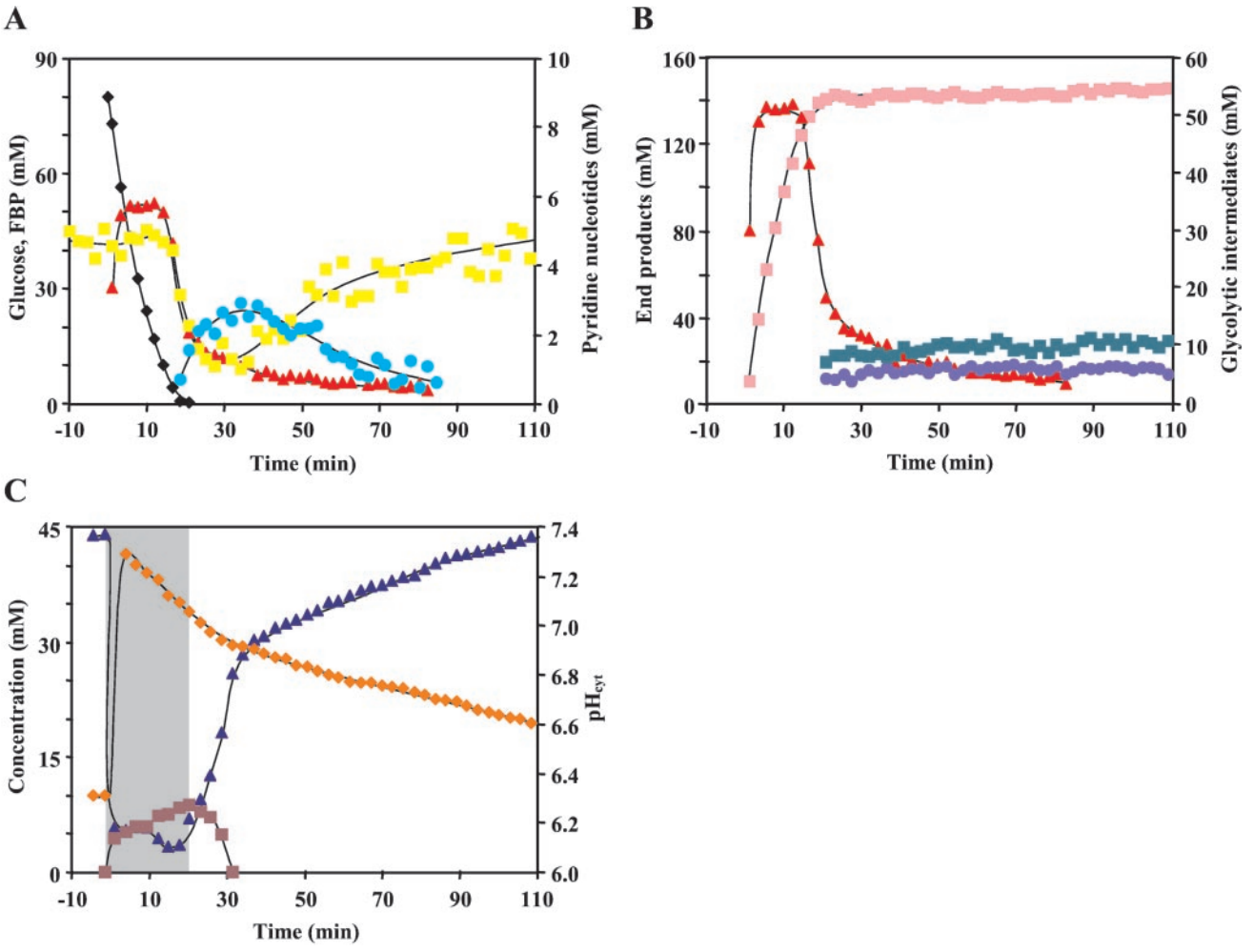

FIG. 3. **Glycolytic dynamics of *L. lactis* MG1363 under anaerobic conditions assessed using *in vivo* ^{13}C and ^{31}P NMR.** Consumption of [1-^{13}C]glucose (80 mM) and evolution of FBP, NAD$^+$, and NADH (*A*) and lactate, FBP, 3-PGA, and PEP (*B*) monitored by ^{13}C NMR is shown. Biochemical parameters determined by ^{31}P NMR during the metabolism of glucose (80 mM) is shown. *Black diamond*, glucose; *pink square*, lactate; *red triangle*, FBP; *green square*, 3-PGA; *blue circle*, PEP; *yellow square*, NAD$^+$; *aqua circle*, NADH; *burgundy square*, NTP; *blue triangle*, P$_i$; *orange diamond*, intracellular pH. The *shaded area* indicates glucose availability. *Fitted lines* are simple interpolations.

evaluated both by ^{13}C NMR and ^{1}H NMR spectroscopy, and no contaminants were detected in a 3.5 mM [5-^{13}C]nicotinic acid solution (data not shown).

A ^{13}C spectrum of an anaerobic cell suspension of MG1363 cells grown on [5-^{13}C]nicotinic acid is shown in Fig. 1*A*. The spectrum showed a single ^{13}C resonance at 129.1 ppm, tentatively assigned to C$_5$ of NAD$^+$ by comparison with ^{13}C NMR spectra of standards of NAD$^+$, NADH, NADP$^+$, and nicotinic acid (all at 20 mM in 50 mM KP$_i$ buffer, pH 6.5). Chemical shift values of C$_5$ for the latter compounds were 129.1, 105.8, 129.1, and 124.5 ppm, respectively. To confirm the assignment, an ethanol extract of cells grown on [5-^{13}C]nicotinic acid was prepared. After passage through an anion-exchange column, the fractions containing a ^{13}C resonance at 129.1 ppm were pooled and lyophilized. The resulting sample was analyzed by ^{13}C NMR (Fig. 1*B*), and the resonance at 129.1 ppm was firmly assigned to carbon 5 (C$_5$) of NAD$^+$ by spiking the sample with the pure compound. A ^{1}H NMR spectrum of the same sample confirmed the ^{13}C NMR data (Fig. 1*C*). In addition, analysis of the proton spectrum showed that the NAD$^+$ pool was totally labeled at position C$_5$. No signal due to the ^{12}CH was observed, and the two multiplet resonances (*highlighted* with an *asterisk* in Fig. 1*C*), with half the intensity of the other single proton signals, separated by ~0.60 ppm (coupling constant, J^{13}C-^{1}H = 179 Hz) are due to the methine proton bound to carbon 5 (^{13}C$_5$). No resonance attributable to NADH was detected in the spectrum of starved cells. Resonances due to NADP$^+$ or NADPH were not detected *in vivo* or in ethanol extracts of starved cells, albeit a resonance due to carbon 5 of NAD$^+$ was readily observed. NADP$^+$ is stable in ethanol and at the pH used during the extraction procedure, and therefore, lack of detection due to degradation can be excluded. Despite the existence of a typical NADP$^+$-dependent 6-phosphogluconate dehydrogenase (38), the flux through the pentose phosphate pathway when compared with the glycolytic flux is very low in *L. lactis* (39), and no transhydrogenase activities have ever been reported; hence, NADP(H) concentrations in this organism are expected to be very low and, therefore, not amenable to detection by *in vivo* NMR.

Characterization of Pyridine Nucleotides Kinetics during Anaerobic Metabolism of Glucose by MG1363—A selection of ^{13}C NMR spectra showing the evolution of NAD$^+$ and NADH pools before and after the addition of 80 mM [1-^{13}C]glucose to an anaerobic cell suspension of MG1363 is presented in Fig. 2. Before the addition of glucose, a single resonance at 129.1 ppm was detected and assigned to [5-^{13}C]NAD$^+$. When glucose became limiting (~18 min after addition), a resonance appeared at 105.8 ppm that was assigned to [5-^{13}C]NADH. The kinetics of consumption of glucose, the build-up and consumption of FBP, and evolution of NAD$^+$ and NADH were also monitored (Fig. 3*A*). After glucose addition, the FBP pool increased rapidly, reaching a steady level of 51.1 ± 0.3 mM; before and during this

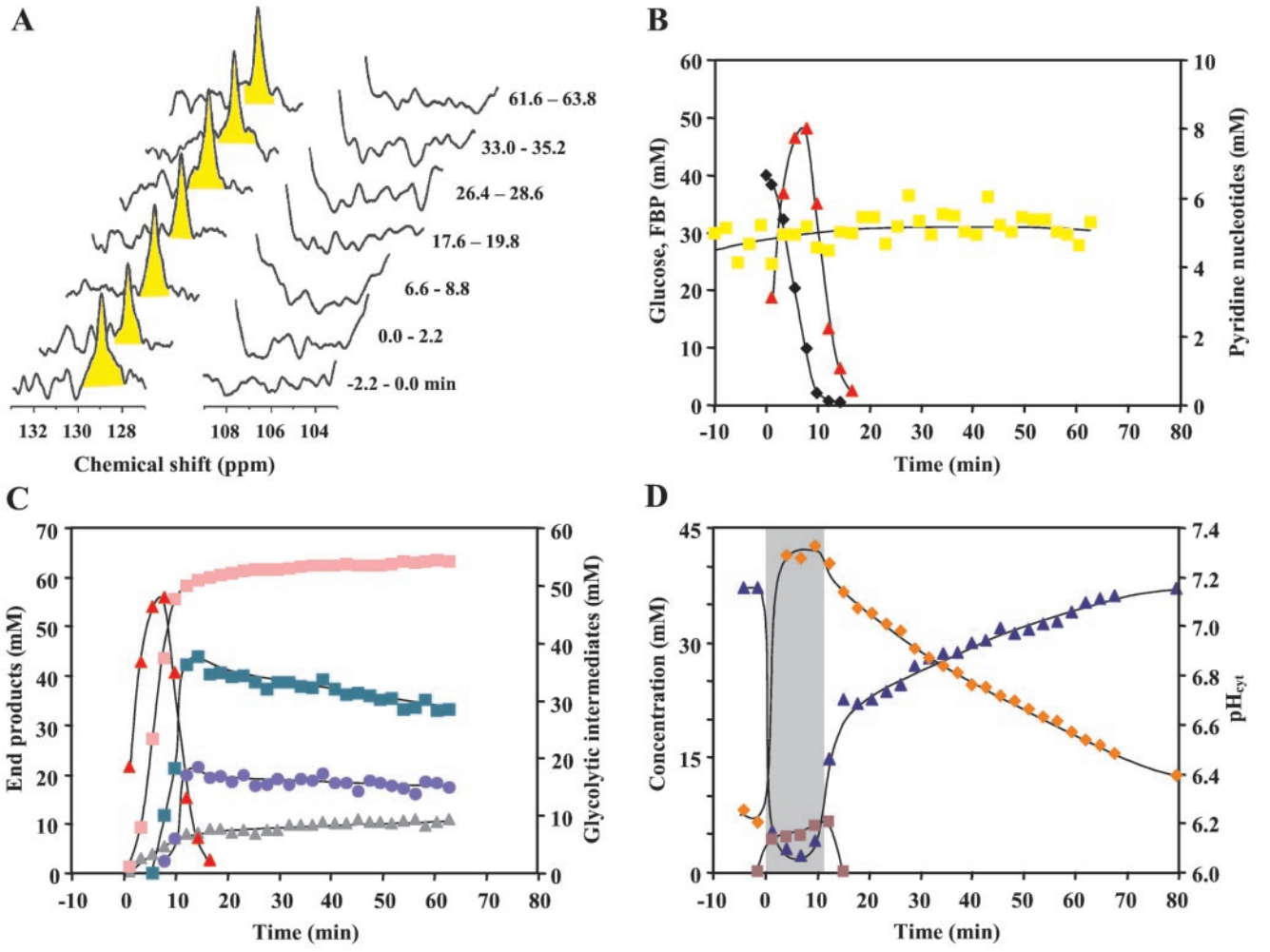

FIG. 4. **Metabolism of glucose (40 mM) in *L. lactis* MG1363 under aerobic conditions at 30 °C, pH 6.5.** Sequence of ^{13}C spectra showing the evolution of NAD^+ (and NADH) pools in MG1363 (grown in chemical defined medium containing 5 mg/liter of [5-^{13}C]nicotinic acid) before and after a glucose pulse under an oxygen atmosphere (*A*). Glucose was added at time 0 min; conditions were similar to those described in Fig. 2. Shown is the time course for the consumption of 40 mM [1-^{13}C]glucose and evolution of FBP, NAD^+, and NADH pools (*B*) and end product formation, FBP, 3-PGA, and PEP pools (*C*) as monitored by ^{13}C NMR and biochemical parameters, determined by ^{31}P NMR during the metabolism of glucose (*D*). *Black diamond*, glucose; *pink square*, lactate; *gray triangle*, acetate; *red triangle*, FBP; *green square*, 3-PGA; *blue circle*, PEP; *yellow square*, NAD^+; *aqua diamond*, NADH; *burgundy square*, NTP; *blue triangle*, P_i; *orange diamond*, intracellular pH. Glucose availability is indicated by the *shaded* area (*D*). Fitted lines are simple interpolations.

TABLE I

End products (mM) from the metabolism of 40 mM glucose by MG1363 and LDH strains under anaerobic or aerobic (100% oxygen saturated) conditions as determined by ^{13}C NMR

Glc_{rate}, glucose consumption rate is expressed in μmol min^{-1} mg of $protein^{-1}$. Mean ± S.D. ($n \geq 2$). ND, not detected. Formate was determined by ^1H NMR.

Products	MG1363		LDH$^-$	
	Anaerobic	Aerobic	Anaerobic	Aerobic
Lactate	73.5 ± 2.3	64.0 ± 1.1	17.7 ± 0.2	0.7 ± 0.0
Acetate	0.5 ± 0.1	10.2 ± 0.8	3.2 ± 0.5	14.2 ± 0.2
Ethanol	0.1 ± 0.0	ND	15.9 ± 0.4	ND
Acetoin	0.1 ± 0.0	0.3 ± 0.2	2.5 ± 0.1	26.1 ± 0.2
2,3-Butanediol	0.2 ± 0.0	0.03 ± 0.0	16.4 ± 0.2	0.7 ± 0.2
Diacetyl	ND	ND	ND	0.24 ± 0.0
Formate	0.66 ± 0.07	ND	18.1 ± 1.3	ND
Glc_{rate}	0.35 ± 0.02	0.22 ± 0.01	0.05 ± 0.01	0.14 ± 0.01

steady state period, no changes were observed in the NAD^+ level, which was maintained at ~4.7 ± 0.3 mM. At the onset of glucose exhaustion, the NAD^+ dropped to 1.4 ± 0.1 mM, whereas the FBP pool declined sharply, and the NADH pool increased from undetectable levels to a maximum of 2.7 ± 0.3 mM. Also, the 3-PGA and PEP pools started to increase, leveling off at 9.2 ± 0.7 and 5.6 ± 0.4 mM, respectively (Fig. 3*B*). Subsequently, the FBP decline slowed down, the NAD^+ pool recovered very slowly to its initial concentration, and the NADH pool became undetectable.

It is well known that NMR is able to detect freely mobile metabolites and that cofactors tightly bound to macromolecules originate very broad lines that are not detected. To assess the extent of detection achieved by *in vivo* NMR, the pool of NAD^+ was also quantified in ethanol extracts of cell suspensions grown under anaerobic conditions (see "Materials and Methods"). We found an NAD^+ concentration of 4.2 ± 0.7 mM (av-

TABLE II
Comparison of enzyme activities determined in crude cell extracts of the MG1363 and LDH⁻ strains grown under anaerobic or aerobic conditions

Enzyme activities are expressed in μmol min^{-1} mg of protein^{-1}. Mean ± S.D. deviation ($n \geq 6$). ND, not detected; —, not determined.

	MG1363		LDH⁻	
	Anaerobic	Aerobic	Anaerobic	Aerobic
Lactate dehydrogenase	30.6 ± 0.2	6.9 ± 1.0	ND	ND
Mt11P dehydrogenase	ND	—	2.0 ± 0.1	0.25 ± 0.00
NADH oxidase	0.06 ± 0.0	0.21 ± 0.01	0.05 ± 0.00	0.07 ± 0.00

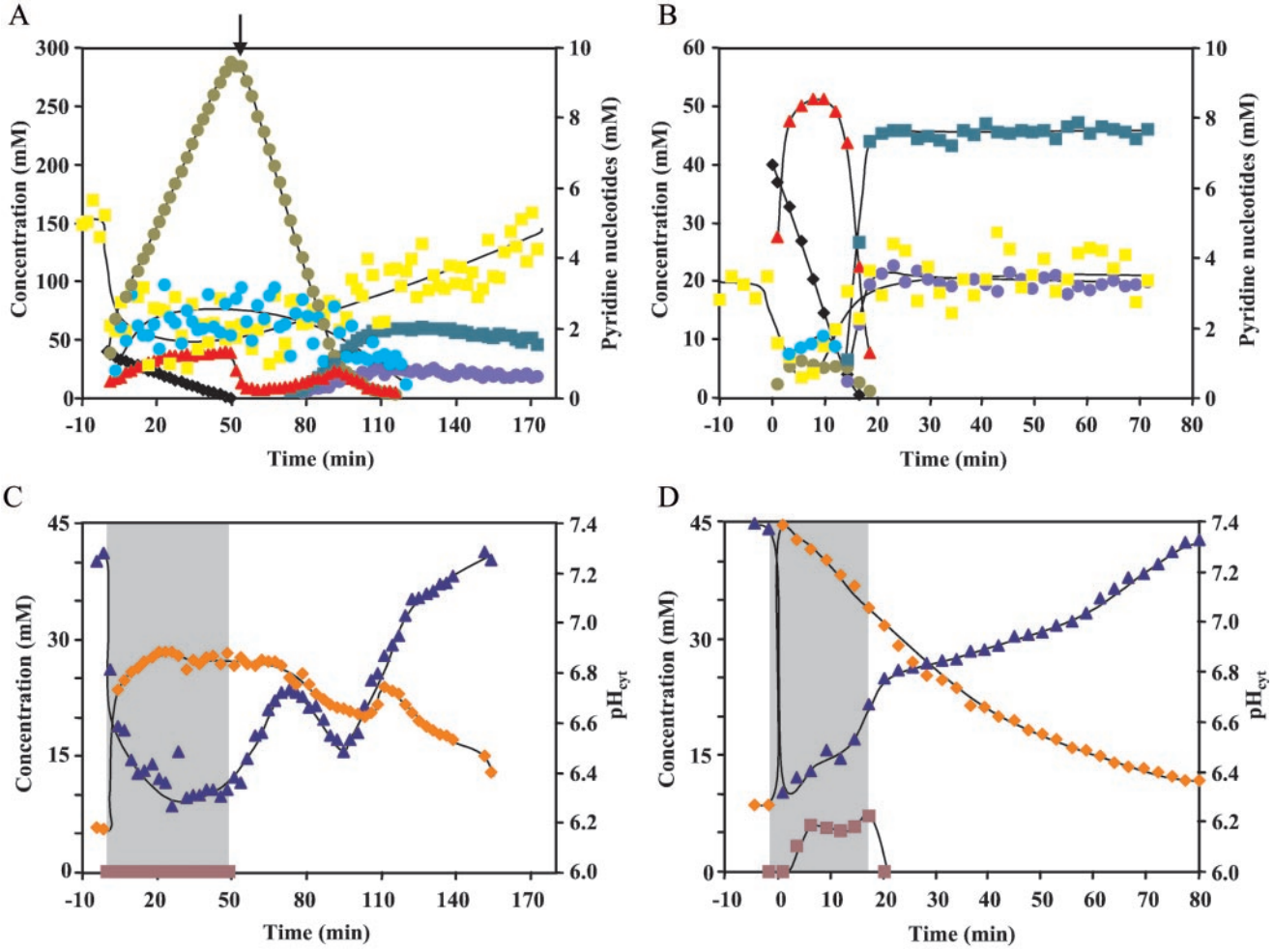

FIG. 5. **Metabolism of glucose (40 mM) in the LDH⁻ strain.** Shown are [1-^{13}C]glucose consumption, FBP, mannitol/Mtl1P, and pyridine nucleotide pools evolution, as determined by ^{13}C NMR under anaerobic (*A*) or aerobic (*B*) conditions, and biochemical parameters, determined by ^{31}P NMR during the metabolism of glucose under anaerobic (*C*) or aerobic (*D*) conditions. *Black diamond*, glucose; *red triangle*, FBP; *green square*, 3-PGA; *blue circle*, PEP; *green circle*, mannitol + mannitol 1-phosphate; *yellow square*, NAD$^+$; *aqua circle*, NADH; *burgundy square*, NTP; *blue triangle*; P$_i$, *orange diamond*, intracellular pH. For the calculations, mannitol was assumed intracellular. The *black arrow* indicates the depletion of mannitol (*A*). Glucose availability is indicated by the *shaded box* (*C* and *D*).

erage of three independent determinations), which compares well with the value measured by *in vivo* NMR. Therefore, the total cell pool of coenzyme is visible by NMR. Also, no evidence for NADH invisibility was found at the different metabolic stages examined since the sum of NAD$^+$ and NADH agreed well with the initial pool of NAD$^+$ in starved cells. The half-height line-width for NAD$^+$ and NADH in the spectra of living cells was 25 and 35 Hz, respectively.

The major product from glucose metabolism under anaerobic conditions was lactate (145.6 ± 0.7 mM), although minor amounts of acetate (1.3 ± 0.1 mM) and 2,3-butanediol (0.3 mM) were detected (not shown). The carbon balance (from glucose) was 95% taking into consideration both extracellular and intracellular metabolites.

The NTP and intracellular P$_i$ levels during the metabolism of glucose (80 mM) as well as the evolution of intracellular pH were determined by ^{31}P NMR (Fig. 3*C*). The concentration of NTP increased from undetectable levels to a maximum of 8.6 ± 0.3 mM, remaining high for a few minutes beyond glucose depletion. After glucose exhaustion (at $t \approx 19.5$ min) a sudden raise of intracellular P$_i$ to about 30 mM was followed by a gradual increase in concentration, reaching values in the range of the initial values (45 mM). We verified that a lower concentration of [1-^{13}C]glucose (40 mM) did not affect the maximum intracellular concentration of FBP nor the general pattern of other intracellular metabolite pools or cytoplasmic pH (data not shown); however, the maximal NTP concentration was lower (~6.1 mM).

Pyridine Nucleotide Levels during Glucose Metabolism Under Aerobic Conditions—A selection of ^{13}C NMR spectra showing the evolution of pyridine nucleotide pools before and after the addition of 40 mM [1-^{13}C]glucose to an aerobic cell suspension of MG1363 (fully saturated in oxygen) is presented in Fig. 4*A*. The intensity of the resonance due to [5-^{13}C]NAD^+ remained constant during the time of observation, and NADH was never detected.

The time courses for glucose consumption, glycolytic intermediates, and NAD^+ evolution are shown in Fig. 4*B*. Intracellular FBP increased to a maximal concentration of 48.2 ± 0.1 mM, and the subsequent decay was considerably steeper than under anaerobic conditions. NAD^+ concentration was constant around 4.8 ± 0.3 mM regardless the presence or absence of glucose, and NADH was always below the detection limit (0.5 mM). The build-up of the 3-PGA and PEP pools, which reached intracellular concentrations of 36.6 ± 1.5 and 15.9 ± 0.4 mM, respectively, was concomitant with the FBP decline upon glucose depletion (Fig. 4*C*).

Under these conditions, a considerable shift from lactate to acetate production was observed (Table I). LDH activity of cells grown under aerobiosis was about half that measured in extracts of cells grown under anaerobiosis, whereas NADH oxidase activity was 3.4-fold higher (Table II).

Biochemical parameters derived from ^{31}P NMR spectra during the metabolism of glucose (40 mM) under aerobic conditions are shown in Fig. 4*D*. The time courses for the variation of intracellular pH, P_i, and NTP were generally similar, except for the decline in NTP after substrate exhaustion, which was clearly faster under aerobic conditions.

Pyridine Nucleotides and Other Intracellular Metabolite Pools in Strain FI9630 (LDH$^-$)—Given the central role played by LDH in the regeneration of NAD^+ during glucose metabolism by *L. lactis*, it was deemed important to measure NAD^+ and NADH pools in an LDH-deficient strain, which has a severely reduced capacity to regenerate NAD^+. Under anaerobic conditions, the NAD^+ was 4.6 ± 0.6 mM before glucose addition and decreased suddenly to 1.9 ± 0.6 mM upon glucose addition, whereas NADH raised from undetectable levels to a mean value of 2.5 ± 0.4 mM (Fig. 5*A*). Meanwhile, the FBP pool increased, reaching a maximal concentration of 36.8 ± 2.3 mM, and the total mannitol pool (Mtl1P and mannitol) raised gradually (maximal concentration 256 ± 7 mM) as long as glucose was available. A similar pattern of glycolytic intermediates was previously reported for *L. lactis* FI7851, a distinct LDH-deficient strain that also uses the reduction of fructose 6-phosphate to Mtl1P as a rescue pathway to regenerate NAD^+ (10). Likewise, in this LDH$^-$ construct, all the mannitol produced was metabolized to the usual end products after glucose exhaustion. Mannitol depletion (at time 73.7 min) and consumption of Mtl1P caused a slow decrease in the NADH levels, which became undetectable after Mtl1P exhaustion. The reverse trend was observed for the NAD^+ pool, which slowly recovered to its initial average value of 4.6 ± 0.6 mM. The buildup of 3-PGA and PEP pools was slow and started immediately after mannitol exhaustion, reaching maximal concentrations of 57.0 ± 3.1 and 23.2 ± 0.6 mM, respectively; these concentrations are significantly higher than those observed for MG1363.

In contrast to MG1363, an oxygen atmosphere was not sufficient to maintain a constant NAD^+ pool in the LDH$^-$ strain; NAD^+ dropped from 3.5 ± 0.6 to 1.2 ± 0.5 mM shortly after glucose addition (Fig. 5*B*). NADH raised from undetectable levels to ~1.5 ± 0.6 mM. FBP and mannitol/Mtl1P increased rapidly to maximal concentrations of 50.1 ± 0.9 and 5.7 ± 0.4 mM. Both NAD^+ and NADH pools returned to their initial state at the time FBP started to decline. Simultaneously, 3-PGA and PEP raised to maximal values of 45.7 ± 0.6 and 21.2 ± 1.8 mM, respectively. No enhancement of NADH oxidase activity was detected in extracts of LDH$^-$ cells grown under aerobiosis. Additionally, Mtl1P dehydrogenase activity, which acts as an alternative enzyme in NAD^+ regeneration, was strongly depressed (about 8-fold) in oxygen grown cells (Table II). Surprisingly, NTP was not detected during glucose consumption by the LDH$^-$ strain under anaerobic conditions, and the intracellular pH did not surpass 6.8 (Fig. 5*C*). Under aerobic conditions, NTP reached a maximal concentration of 6.8 ± 0.2 mM, decreasing to undetectable values immediately after glucose exhaustion, and the profile of intracellular pH was similar to that of MG1363 (Fig. 5*D*). Regardless of the gas atmosphere, the intracellular P_i levels were considerably higher than those observed during glucose consumption by MG1363, implying a stronger inhibitory effect on PK.

Pattern of End Products Derived from the Metabolism of Glucose in Strain FI9630 (LDH$^-$)—A comparison of end products and glucose consumption rates during the metabolism of [1-^{13}C]glucose (40 mM) by the LDH$^-$ and parent strains under anaerobic or aerobic conditions is shown in Table I. Under anaerobiosis, the LDH$^-$ strain produced a mixture of ethanol, formate, 2,3-butanediol, and also lactate; however, no LDH activity could be detected using the standard spectrophotometric assay coupled to NADH oxidation (Table II). We propose that an alternative LDH with different kinetic parameters must be responsible for lactate production; in fact, three other putative *ldh* genes were found in the genome of *L. lactis* IL1403 (2). In the LDH$^-$ strain, lactate production was severely inhibited under aerobic conditions, and glucose metabolism was switched toward the production of acetoin and acetate. Significant amounts of the flavor compound diacetyl were observed as well. Pyruvate accumulation was detected in the LDH$^-$, the concentration being 2.5-fold higher under aerobic conditions (5.8 ± 0.3 mM). Under anaerobic conditions, aspartate production was observed in MG1363 (5.2 ± 0.4 mM) and in the LDH$^-$ (10.8 ± 0.4 mM). The presence of oxygen induced a 2-fold increase in the concentration of aspartate and accumulation of citrate up to 2.6 ± 0.2 and 33.3 ± 0.6 mM in MG1363 and the LDH$^-$ strain, respectively.

Under anaerobic conditions the glucose consumption rate of the LDH$^-$ strain was 7-fold lower than that of the parent strain, whereas under aerobic conditions the glucose consumption rate was only 2-fold lower (Table I). The growth rate of this strain was 0.70 h^{-1}, whereas strain MG1363 had growth rates of 1.15 and 1.00 h^{-1} under anaerobic or aerobic conditions, respectively. The lower consumption rate of glucose by LDH$^-$ reflects the difficulty to oxidize NADH. Under aerobic conditions, regeneration of NAD^+ by NADH oxidases relieves this obstruction, allowing for a faster glucose uptake.

Regulation of LDH and GAPDH by NAD^+ and NADH—The effect of the NADH/NAD^+ ratio on GAPDH and LDH activities (forward reactions) was investigated using crude cell extracts prepared from cell suspensions of MG1363 grown under anaerobiosis. Maximal activities of 30.6 ± 0.6 and 29.7 ± 0.8 μmol min^{-1} mg of $protein^{-1}$ were determined for LDH and GAPDH, respectively. LDH activity was not affected by the NADH/NAD^+ ratio, when a constant NAD^+ concentration (5 mM) was used and the concentration of NADH varied between 0 and 0.5 mM. The NAD^+ concentration was set at 5 mM to mimic the maximal pool of this metabolite determined *in vivo* in *L. lactis*. Conversely, when NADH was set constant (0.3 or 0.5 mM) and the NAD^+ concentration was varied between 0 and 10 mM, the LDH activity decreased as the concentration of NAD^+ increased.

Equivalent data for GAPDH were obtained; setting NADH at

a constant level resulted in a specific degree of inhibition, which was independent of the NADH/NAD^+ ratio. We concluded that under the conditions examined inhibitory effects on LDH and GAPDH were due to NAD^+ or NADH concentrations, respectively, rather than the NADH/NAD^+ ratio. At the maximal physiological NAD^+ concentration (~5 mM) and disregarding other possible effectors, about 50% of the maximal LDH activity was retained. GAPDH activity was 50% inhibited by 0.4 mM NADH, meaning that the activity of this enzyme *in vitro* would be severely inhibited when the NADH concentration rises to values such as those detected *in vivo* in the present study.

DISCUSSION

It is generally accepted that pyridine nucleotides play a key role in metabolic control and that reliable data on their pool sizes are essential for an accurate description of cell metabolism. In this work we used *in vivo* ^{13}C NMR to determine NADH and NAD^+ levels in *L. lactis*. Despite the disadvantage of a low sensitivity that hampers determinations in growing cultures, this technique has invaluable advantages: in a single sample, reduced and oxidized forms of pyridine nucleotides can be quantified on line along with glycolytic intermediates and end products. Furthermore, information on levels of NTP, intracellular pH, and inorganic phosphate is accessible from experiments monitored by ^{31}P NMR; in this way, it was possible to obtain a global picture of glucose metabolism in *L. lactis* in real time through the measurements of several intracellular parameters *in vivo*.

NAD^+ was constant and maximal during glucose metabolism in the parent strain, but at the onset of glucose depletion and under anaerobic conditions, it decreased sharply with a concomitant increase of NADH. Under aerobic conditions, however, the NAD^+ level remained maximal throughout all the stages. Therefore, we conclude that when glucose was not limiting and metabolism proceeded at a full rate, LDH activity alone (under anaerobic conditions) was sufficient to promptly oxidize NADH formed by GAPDH, leading to a quasi-steady state condition where the level of NAD^+ remained maximal. However, when glucose became limiting, there was a sharp decline in NAD^+ and a consequent rise of NADH, attributed to the decrease in the flux through LDH, the main site for NADH oxidation under anaerobic conditions. This decrease in flux through LDH resulted directly from the reduced availability of the substrate, pyruvate, caused by (i) cessation of glucose transport via the PEP-phosphotransferase system, which releases pyruvate efficiently, and (ii) inhibition of PK by the combined action of high levels of P_i, which accumulates at this stage, and decreased levels of FBP. The antagonistic effects of FBP and P_i in the modulation of PK activity have been put forward by other authors (40, 41).

NADH oxidase activity present in *L. lactis* provided an extra route for the oxidation of NADH, when oxygen was available. Therefore, under aerobic conditions, the NAD^+ level was maximal, regardless of glucose being available or exhausted or, in other words, regardless of PK inhibition; the activity of NADH oxidase allowed for an efficient regeneration of NAD^+, counteracting the constriction of flux through PK (and consequently through LDH).

In the construct with a disruption in the *ldh* gene, the NAD^+ pool dropped sharply immediately after the supply of glucose regardless of anaerobic or aerobic conditions (Fig. 5), showing that NADH oxidase activity was insufficient to compensate for the severe LDH deficiency. A proportional increase in NADH concentration was observed, which reached 2.5 mM under anaerobic conditions and up to 1.5 mM in the presence of oxygen. Under anaerobic conditions, the glycolytic flux was strongly depressed (7-fold lower than that of the parent strain, MG1363), but interestingly, in the presence of oxygen the glucose consumption rate increased significantly, amounting to 60% that of MG1363. This result clearly shows that a high glycolytic flux is compatible with a high concentration of NADH in the cell (higher than 1 mM and higher than the concentration of NAD^+, Fig. 5); this concentration would inhibit GAPDH to a considerable extent on the basis of *in vitro* data for this enzyme (Supplemental Fig. 1). Therefore, it appears that GAPDH activity *in vivo* is not as sensitive to inhibition by NADH as *in vitro* (Ref. 36 and this study) or that the excess activity of the enzyme in the cell allows for a residual flux comparable with that of the parental strain even when the extent of inhibition is extremely high. In fact, we have found about 100-fold excess GAPDH activity in extracts of MG1363.

The strong accumulation of FBP during the initial stage of glucose metabolism (activation stage) is a feature common to all the strains and conditions examined. Immediately before glucose addition the level of P_i is invariably high; therefore, PK is expected to be virtually inoperative. As a consequence of this initial bottleneck, FBP builds up at the expense of the P_i pool, resulting in the relief of PK inhibition and the establishment of a quasi-steady state characterized by a constant level of FBP (in the 50 mM range) and maximal rate of glucose consumption. This high FBP level was important to counteract the negative effect of P_i on PK, allowing for reasonably high flux even at high intracellular P_i concentration.

At the onset of glucose depletion, a reversion of the events occurring during the activation stage was observed. FBP was depleted at a rate dependent on the cell capacity to regenerate NAD^+ (higher rate under aerobic conditions), and the pool of P_i increased sharply, resulting in the inhibition of PK. This constriction was responsible for the strong accumulation under aerobic conditions of 3-PGA and PEP derived from the metabolism of residual FBP; in fact, when oxygen is available, NADH oxidases provide an alternative pathway for the regeneration of NAD^+, which disregards PK, thus enabling the build up of 3-PGA and PEP pools to higher levels and the fast depletion of FBP (compare Figs. 3*B* and 4*C*). In this respect, the behavior of the LDH^- strain deserves further comment, since the levels of 3-PGA and PEP were high even under anaerobic conditions despite the low intrinsic capacity of this strain to oxidize NADH upstream the pyruvate node; in this case, oxidation of NADH after glucose depletion was coupled to reduction of acetoin, as evidenced by the decline in the concentration of this end product (Supplemental Fig. 2).

In all cases examined the maximum level of NTP was around 6–7 mM, except for the LDH^- strain under anaerobic conditions in which NTP was too low to be detected *in vivo* (less than 1 mM). It is likely that the NTP formed was rapidly used to maintain transmembrane gradients in this mutant strain, which has considerably reduced rates of lactate production and efflux. As a consequence of this low energizing level, the intracellular pH during glucose metabolism was also lower (by about 0.4 pH units) than in the parent strain.

The presence of a bottleneck at the level of LDH in the LDH-deficient strain was also evidenced by the clear accumulation of pyruvate and aspartate. The limited capacity to oxidize NADH led to the accumulation of this coenzyme (up to 2.5 mM), which forced the operation of the rescue pathway to oxidize NADH through Mtl1P dehydrogenase with production of mannitol (10). The accumulation of pyruvate, only observed in this strain, indicates flux constriction at pyruvate-utilizing enzymes rather than at the level of GAPDH that could be severely inhibited by the high NADH content.

The comparison of the metabolic profiles of the LDH^- strain

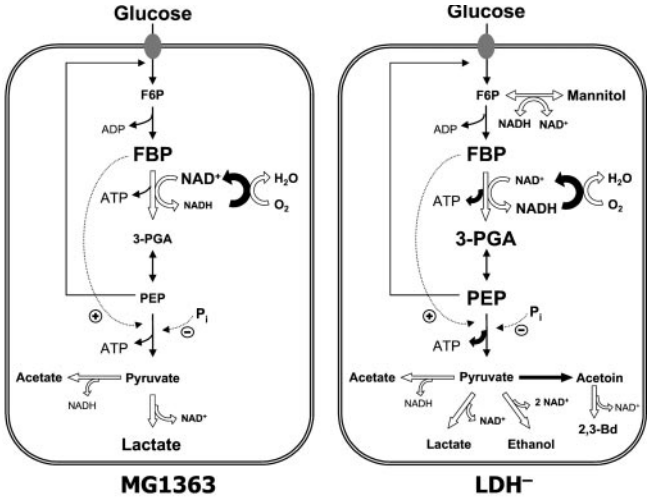

FIG. 6. **Overview of main metabolic features observed for *L. lactis* MG1363 and the mutant deficient in LDH, highlighting major regulation sites invoked under "Discussion."** Case sizes are intended to reflect pool sizes. *Stripped arrows* indicate steps activated under aerobic conditions. *Plus* and *minus* signs refer to positive or negative effectors of enzyme activities. *2,3-Bd*, 2,3-butanediol; *F6P*, fructose-6-phosphate.

under anaerobic and aerobic conditions is particularly informative. The presence of oxygen induces a remarkable increase in the glycolytic flux (3-fold) despite the high NADH and P_i (>10 mM) concentrations observed during the utilization of glucose. The results suggest that when glucose is not limiting, the flux through GAPDH is relatively insensitive to NADH levels as high as 1.5 mM, and there is lack of evidence for strong toxicity associated with NADH concentrations in this range. Moreover, it is interesting to point out the substantial flux sustained via PK despite the high level of P_i (Fig. 5), a known inhibitor of the enzyme. The absence of significant constriction at this enzymatic step is further supported by the inability to detect 3-PGA and PEP in fully active cells and by the higher concentrations of pyruvate, aspartate, and citrate that accumulated under aerobiosis, a direct consequence of pyruvate accumulation due the higher glycolytic flux. An overview of the main metabolic features of the MG1363 and the LDH-deficient construct is shown in Fig. 6.

Recent work using a series of mutant strains of *L. lactis* with a wide range of LDH activities has shown convincingly that LDH has no control on the glycolytic flux, reflecting the excess capacity of this pivotal enzyme in the cell (42). Manipulation of the PFK activity, however, had a negative effect on the glycolytic flux, but the interpretation of results is complicated by co-lateral effects on the activity of the other enzymes encoded by the *las* operon (43). It has been shown that the *in vitro* activities of the two main dehydrogenases in *L. lactis* are highly sensitive to the levels of NADH or NAD^+, and the NADH/NAD^+ ratio has been proposed to play a predominant role in the control of flux through glycolysis (7). Our *in vivo* measurements of intracellular pools of pyridine nucleotides and several other metabolites in MG1363 show that under steady state conditions of glucose metabolism, NADH was kept at undetectable levels by the luxurious LDH activity in the wild type strain. Thus, it is unlikely that the control of the glycolytic flux resides primarily at the level of GAPDH, since the activity of this enzyme was sufficient to support a high flux even at concentrations of NADH in the range of 1.5 mM. It is conceivable that, as for the other main dehydrogenase (LDH), the activity of GAPDH in the cell is in great excess, because the activities of LDH and GAPDH measured *in vitro* in MG1363 and other strains are comparable (this study and Ref. 13). On the other hand, overproduction of PK in *L. lactis* did not lead to enhancement of the glycolytic flux.[2] At this point we speculate that glycolytic flux could be controlled by ADP availability or ATP surplus, as previously proposed for yeast and other organisms (31, 44–47). High levels of ATP were determined in *L. lactis*, but ADP was not detected in ^{31}P NMR spectra of starved cells, suggesting restricted motion, probably due to binding to proteins (48). Therefore, it is conceivable that the free ADP pool could be a limiting factor when glucose is abundant.

Despite the fact that a final answer to the complex question of what controls glycolytic flux in *L. lactis* cannot be given at this stage, it is clear that our data do not support the existence of major control at the level of GAPDH in the wild type strain. The unique *in vivo* measurements accomplished in this work provided an interpretation of glucose metabolism based on direct observations rather than on unreliable extrapolations from *in vitro* data or speculative reasoning derived from the pattern of end products. Although a more substantiated proposal cannot be put forward, we favor the view that glycolytic control resides mainly outside glycolysis, probably in the processes that affect the ATP and/or ADP content rather than the NADH/NAD^+ ratio.

Acknowledgment—We thank A. Mingote for technical assistance in the purification of NAD^+.

REFERENCES

1. de Vos, W. M. (1999) *Curr. Opin. Microbiol.* **2,** 289–295
2. Bolotin, A., Wincker, P., Mauger, S., Jaillon, O., Malarme, K., Weissenbach, J., Ehrlich, S. D., and Sorokin, A. (2001) *Genome Res.* **11,** 731–753
3. Cocaign-Bousquet, M., Garrigues, C., Loubiere, P., and Lindley, N. D. (1996) *Antonie Van Leeuwenhoek* **70,** 253–267
4. Thomas, T. D., Ellwood, D. C., and Longyear, V. M. (1979) *J. Bacteriol.* **138,** 109–117
5. Condon, S. (1987) *FEMS Microbiol. Rev.* **46,** 269–280
6. Thomas, T. D. (1976) *J. Bacteriol.* **125,** 1240–1242
7. Garrigues, C., Loubiere, P., Lindley, N. D., and Cocaign-Bousquet, M. (1997) *J. Bacteriol.* **179,** 5282–5287
8. Poolman, B., Bosman, B., Kiers, J., and Konings, W. N. (1987) *J. Bacteriol.* **169,** 5887–5890
9. Lopez de Felipe, F., Kleerebezem, M., de Vos, W. M., and Hugenholtz, J. (1998) *J. Bacteriol.* **180,** 3804–3808
10. Neves, A. R., Ramos, A., Shearman, C., Gasson, M. J., Almeida, J. S., and Santos, H. (2000) *Eur. J. Biochem.* **267,** 3859–3868
11. Hols, P., Ramos, A., Hugenholtz, J., Delcour, J., de Vos, W. M., Santos, H., and Kleerebezem, M. (1999) *J. Bacteriol.* **181,** 5521–5526
12. Garrigues, C., Goupil-Feuillerat, N., Cocaign-Bousquet, M., Renault, P., Lindley, N. D., and Loubiere, P. (2001) *Metab. Eng.* **3,** 211–217
13. Even, S., Lindley, N. D., and Cocaign-Bousquet, M. (2001) *J. Bacteriol.* **183,** 3817–3824
14. Jensen, N. B. (1999) *Influence of Oxygen on Growth and Product Formation in Lactic Acid Bacteria.* Ph.D. thesis, Department of Biotechnology, Technical University of Denmark, Lyngby, Denmark
15. Snoep, J. I. (1992) *Regulation of Pyruvate Catabolism in Enterococcus faecalis. A Molecular Approach to Physiology.* Ph.D. thesis, Department of Microbiology, Biotechnology Centre, University of Amsterdam, Amsterdam, The Netherlands
16. Andersen, K. B., and von Meyenburg, K. (1977) *J. Biol. Chem.* **252,** 4151–4156
17. de Graef, M. R., Alexeeva, S., Snoep, J. L., and Teixeira de Mattos, M. J. (1999) *J. Bacteriol.* **181,** 2351–2357
18. Gonzalez, B., Francois, J., and Renaud, M. (1997) *Yeast* **13,** 1347–1355
19. Leonardo, M. R., Dailly, Y., and Clark, D. P. (1996) *J. Bacteriol.* **178,** 6013–6018
20. London, J., and Knight, M. (1966) *J. Gen. Microbiol.* **44,** 241–254
21. Wimpenny, J. W., and Firth, A. (1972) *J. Bacteriol.* **111,** 24–32
22. Harrison, D. E., and Chance, B. (1970) *Appl. Microbiol.* **19,** 446–450
23. London, R. E. (1988) *Prog. Nucl. Magn. Reson. Spectrosc.* **20,** 337–383
24. Unkefer, C. J., Blazer, R. M., and London, R. E. (1983) *Science* **222,** 62–65
25. Poolman, B., and Konings, W. N. (1988) *J. Bacteriol.* **170,** 700–707
26. Leenhouts, K., Buist, G., Bolhuis, A., ten Berge, A., Kiel, J., Mierau, I., Dabrowska, M., Venema, G., and Kok, J. (1996) *Mol. Gen. Genet.* **253,** 217–224
27. Llanos, R. M., Hillier, A. J., and Davidson, B. E. (1992) *J. Bacteriol.* **174,** 6956–6964
28. Griffin, H. G., Swindell, S. R., and Gasson, M. J. (1992) *Gene* **122,** 193–197
29. Bryson, T. A., Wisowaty, J. C., Dunlap, R. B., Fisher, R. R., and Ellis, P. D. (1974) *J. Org. Chem.* **39,** 1158–1160
30. Vogel, A. I. (1989) *Vogel's Textbook of Practical Organic Chemistry*, 5th Ed., p. 1062, Longman Scientific and Technical, Essex, England

[2] A. Ramos, A. R. Neves, P. Lopez, and H. Santos, unpublished observations.

31. Neves, A. R., Ramos, A., Nunes, M. C., Kleerebezem, M., Hugenholtz, J., de Vos, W. M., Almeida, J., and Santos, H. (1999) *Biotechnol. Bioeng.* **64,** 200–212
32. Santos, H., and Turner, D. L. (1986) *J. Magn. Reson.* **68,** 345–349
33. Ramos, A., Boels, I. C., de Vos, W. M., and Santos, H. (2001) *Appl. Environ. Microbiol.* **67,** 33–41
34. Poolman, B., Smid, E. J., Veldkamp, H., and Konings, W. N. (1987) *J. Bacteriol.* **169,** 1460–1468
35. Bradford, M. M. (1976) *Anal. Biochem.* **72,** 248–254
36. Even, S., Garrigues, C., Loubiere, P., Lindley, N. D., and Cocaign-Bousquet, M. (1999) *Metab. Eng.* **1,** 198–205
37. Penfound, T., and Foster, J. W. (1996) in *Escherichia coli and Salmonella: Cellular and Molecular Biology*, 2nd Ed., pp. 721–730, American Society for Microbiology, Washington, D. C.
38. Tetaud, E., Hanau, S., Wells, J. M., Le Page, R. W., Adams, M. J., Arkison, S., and Barrett, M. P. (1999) *Biochem. J.* **338,** 55–60
39. Nóvak, L., and Loubiere, P. (2000) *J. Bacteriol.* **182,** 1136–1143
40. Thompson, J., and Torchia, D. A. (1984) *J. Bacteriol.* **158,** 791–800
41. Mason, P. W., Carbone, D. P., Cushman, R. A., and Waggoner, A. S. (1981) *J. Biol. Chem.* **256,** 1861–1866
42. Andersen, H. W., Pedersen, M. B., Hammer, K., and Jensen, P. R. (2001) *Eur. J. Biochem.* **268,** 6379–6389
43. Andersen, H. W., Solem, C., Hammer, K., and Jensen, P. R. (2001) *J. Bacteriol.* **183,** 3458–3467
44. Koebmann, B. J., Pedersen, M. B., Nilsson, D., and Jensen, P. R. (2000) in *BTK2000: Animating the Cellular Map* (Hofmeyr, J., Rohwer, J. M., Snoep, J. L., eds) Proceedings of the Ninth International BioThermoKinetics Meeting, pp. 299–306, Stellenbosch University Press, Stellenbosch, South Africa
45. Teusink, B., Walsh, M. C., van Dam, K., and Westerhoff, H. V. (1998) *Trends Biochem. Sci.* **23,** 162–169
46. Larsson, C., Nilsson, A., Blomberg, A., and Gustafsson, L. (1997) *J. Bacteriol.* **179,** 7243–7250
47. Ricci, J. C. D. (2000) *Biochem. Biophys. Res. Commun.* **271,** 244–249
48. Hutson, S. M., Berkich, D., Williams, G. D., LaNoue, K. F., and Briggs, R. W. (1989) *Biochemistry* **28,** 4325–4332